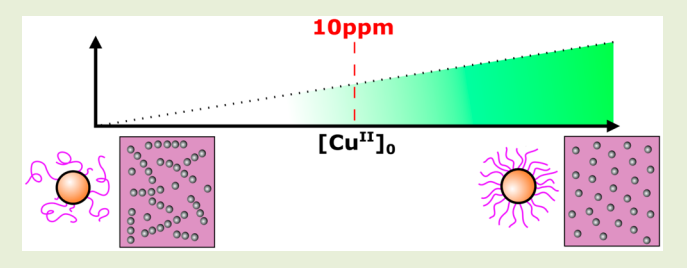
Control of Dispersity and Grafting Density of Particle Brushes by Variation of ATRP Catalyst Concentration

Zongyu Wang,^{†,‡} Jiajun Yan,^{†,‡,§} Tong Liu,[†] Qiangbing Wei,^{†,||} Sipei Li,[†] Mateusz Olszewski,[†] Jianing Wu,[⊥] Julian Sobieski,[†] Marco Fantin,[†] Michael R. Bockstaller,*,[⊥] and Krzysztof Matyjaszewski*, † ®

Supporting Information

Downloaded via CARNEGIE MELLON UNIV on December 20, 2019 at 02:28:47 (UTC). See https://pubs.acs.org/sharingguidelines for options on how to legitimately share published articles.

ABSTRACT: Silica particles with grafted poly(methyl methacrylate) brushes, SiO₂-g-PMMA, were prepared via activator regeneration by electron transfer (ARGET) atom transfer radical polymerization (ATRP). The grafting density and dispersity of the polymer brushes was tuned by the initial ATRP catalyst concentration ([CuII/L]0). Sparsely grafted particle brushes, which also displayed an anisotropic stringlike structure in TEM images, were obtained at very low catalyst concentrations, $[Cu^{II}/L]_0 < 1$ ppm. The effect of the



initial catalyst concentration on dispersity and initiation efficiency in the particle brush system was similar to that observed in the synthesis of linear PMMA homopolymers. The kinetic study revealed a transition from controlled radical polymerization to a less controlled process at low monomer conversion, when the [Cu^{II}/L]₀ decreased below about 10 ppm.

olymer brushes have been extensively investigated over the past 50 years because they are effective particle/ surface modifiers.¹⁻⁶ Brushes are dense layers of polymer chains with a chain end attached to a surface. Both theory and simulations were used to understand how brush heights and grafting densities affect the properties of nanocomposite hybrid materials.7 The preparation of "monodisperse" brushes (brushes with a very narrow molecular weight distribution) requires well controlled synthetic methods. Atom transfer radical polymerization (ATRP), a powerful controlled radical polymerization technique, has produced a vast array of polymeric materials with excellent control over topologies, compositions, microstructures, and functionalities over the past two decades. 3,5,8-10 Recently, the concentration of Cu-based catalysts can be diminished to the ppm level with the use of reducing agents and the rational selection of suitable Cucomplexing ligands in activator regeneration by electron transfer (ARGET) ATRP technique. 11-14

Graft density and uniformity of polymer chains can significantly affect conformation of polymer brushes and the properties of composite systems. 15 Theoretical studies showed that polymer brushes exhibit a relaxation of chain extended conformation with increasing molecular weight. Also, higher dispersity can stabilize dispersions, even if the average graft molecular weight is lower than the matrix molecular weight. 16 Moreover, simulations demonstrated that dispersity may affect adhesion of microscale particles by enhancing interparticle entanglement. $^{16-18}$ Brushes with higher dispersity may significantly improve the ability and efficacy of smart coatings, as compared to monodisperse brushes. 19,20 Recent reports demonstrated that particle brushes with bimodal molecular weight distribution (MWD) showed superior mechanical properties and significantly improved interparticle and particle-matrix interactions. 21-25 However, some conventional approaches to broaden MWD might be complicated and difficult to perform. In this contribution, we report the synthesis of SiO₂-g-PMMA particle brushes with controlled dispersity and grafting density using a facile scalable approach consisting of simple tuning of the initial ATRP catalyst concentration, top scheme in Figure 1. A similar approach was used for liner chains in ARGET ATRP. 26-28

The effect of varying the initial concentration of catalyst [Cu^{II}/L]₀ on the grafting density and dispersity of SiO₂-g-PMMA particle brushes synthesized with ARGET ATRP was studied. A fixed concentration of initiating sites on SiO₂-Br particles (200 ppm) and a wide range of catalyst (CuBr₂/ Me_6TREN) concentrations ($[Cu^{II}/L]_0 = 0.01 \sim 400 \text{ ppm}$) in 50% v/v solvent (anisole) at 60 °C was applied, and the results

Received: May 28, 2019 Accepted: June 21, 2019 Published: June 25, 2019

Department of Chemistry, Carnegie Mellon University, 4400 Fifth Avenue, Pittsburgh, Pennsylvania 15213, United States

 $^{^\}perp$ Department of Materials Science and Engineering, Carnegie Mellon University, 5000 Forbes Avenue, Pittsburgh, Pennsylvania 15213, United States

Key Laboratory of Eco-Environmental-Related Polymer Materials, Ministry of Education, College of Chemistry and Chemical Engineering, Northwest Normal University, Lanzhou 730070, China

ACS Macro Letters

Letter

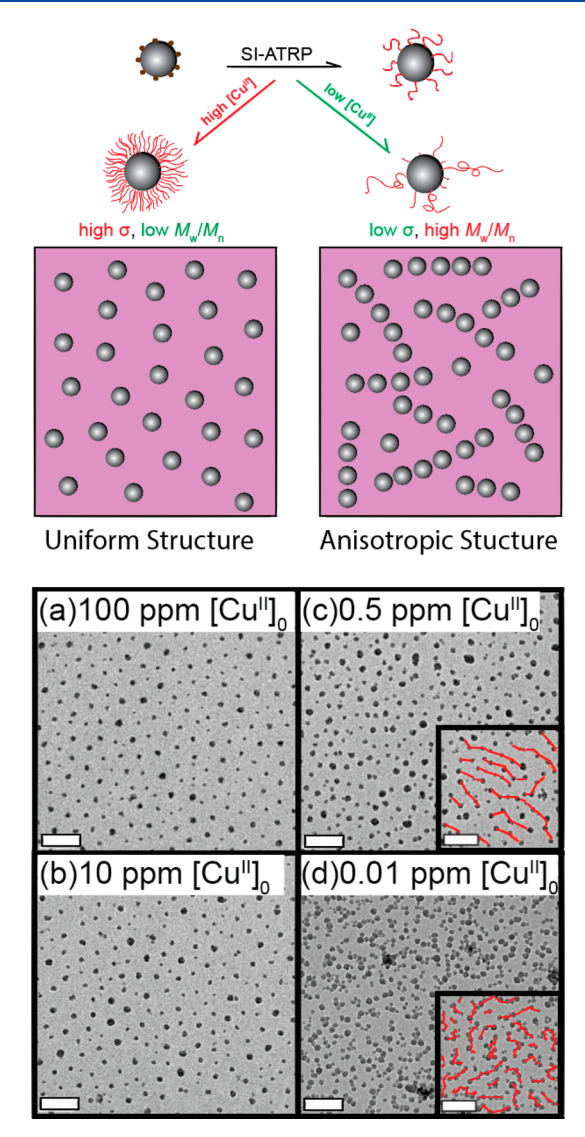


Figure 1. Schematic graph of the synthesis of SiO₂-*g*-PMMA particle brushes with different initial catalyst concentrations and TEM images of monolayer films of SiO₂-*g*-PMMA particle brushes with different DP and grafting densities. (a) PMMA-3, DP = 600, $M_{\rm w}/M_{\rm n}$ = 1.16, σ = 0.65 nm⁻², (b) PMMA-6, DP = 787, $M_{\rm w}/M_{\rm n}$ = 1.46, σ = 0.15 nm⁻², (c) PMMA-10, DP = 2471, $M_{\rm w}/M_{\rm n}$ = 1.90, σ = 0.049 nm⁻², (d) PMMA-15, DP = 1972, $M_{\rm w}/M_{\rm n}$ = 2.06, σ = 0.015 nm⁻². Red lines highlight the string structures in (c) and (d) insets. Scale bar: 100 nm.

are provided in Table 1. Because of the possible gelation of the reaction medium due to interparticle coupling, reactions were carried out for a relatively short time (<2 h) to diminish coupling between nanoparticles (NPs). Figure 2a,b shows the correlation of the grafting density and dispersity with the initial concentration of the catalyst ($[Cu^{II}/L]_0$). The results indicate that the dispersity of the grafted brushes increased with the decreasing initial concentration of the catalyst, from 1.18 to 2.11. On the other hand, the grafting density, which is an indication of the initiation efficiency of the reaction was relatively steady at high catalyst concentrations (>25 ppm), but dropped significantly with lower initial catalyst concentrations at <10 ppm conditions, from 0.71 to 0.012 chain/nm². Such an observation agreed with the previous theoretical study on the correlation between grafting density and dispersity.²⁹ After polymerization, the products were precipitated by the addition

to cold methanol to remove the catalyst (CuBr₂/Me₆TREN), solvent, unreacted monomer, and NPs.

Due to the significant decrease of the grafting density at low catalyst concentrations, it is necessary to verify if the polymer chains were initiated from the surface of silica NPs or via side reactions in the solution (e.g., thermal self-initiation).³⁰⁻³² Therefore, we characterized the samples by TEM to confirm the attachment of polymer brushes to the surface of the NPs. TEM images showed that no obvious free homopolymers were present after polymerization, and all particle brushes were welldispersed on the Cu grids without aggregations, even with catalyst concentration > 0.1 ppm, Figure 1 (cf. also Figure S6). It should be noted that, as the grafting density diminished with the decreasing initial catalyst concentration, the morphologies of particle brushes changed. Above 10 ppm [CuII/L]₀, isotropic and uniform structures were observed (Figure 1a,b). On the other hand, as the [CuII/L]0 decreased below 10 ppm, the grafting density dropped to <0.15 chains/nm², and an anisotropic structure was observed in the TEM images, Figure 1c. This trend further evolved with the decreasing [CuII/L]₀ and grafting density, Figure 1d. These string-like structures, top scheme in Figure 1, were previously reported and studied in sparsely grafted particle systems. 33-35 The driving force to form this self-assembled structure was the attraction between patches of bare surfaces of NPs.³⁶

Due to a short reaction time (1 h) and relatively low conversion (~1%) in several reactions, accurate kinetic plots could not be obtained. Therefore, we conducted a series of homopolymerizations of linear model systems with similar initial catalyst concentrations to study the reaction kinetics. Linear PMMA samples were prepared under the same conditions used to prepare the SiO₂-g-PMMA particle brushes, except for the use of a small-molecule initiator, ethyl 2-bromoisobutyrate (EBiB), and the results are reported in Table 2.

The key factors dominating the dispersity of model linear ATRP reactions can be summarized in the following equation (if contribution of termination is small).^{39–41}

$$\frac{M_{\rm w}}{M_{\rm n}} = 1 + \frac{[{\rm RX}]k_{\rm p}}{k_{\rm d}[{\rm Cu^{II}}]} \left(\frac{2}{p} - 1\right) \tag{1}$$

where [RX] and [Cu^{II}] are the concentrations of the alkyl halide chain end and the Cu^{II} species, respectively; $k_{\rm p}$ and $k_{\rm d}$ are the rate constants of propagation and deactivation, respectively; p is the conversion. [Cu^I]/[Cu^{II}] ratio can be estimated based on the apparent rate constants (Figure S1) of polymerization and the ATRP equilibrium constant, $K_{\rm ATRP}$, using the following equation.

$$k_{\rm p}^{\rm app} = k_{\rm p} K_{\rm ATRP} \frac{[\rm RX][\rm Cu^I]}{[\rm Cu^{II}]} \tag{2}$$

Table 2 and Figure 3 show the correlation between dispersity/initiation efficiency and the initial catalyst concentration in polymerization of linear PMMA homopolymers. Similar trends to those observed in the particle brush system were obtained. In the linear model system control of polymerization decreased with the initial concentration of catalyst. Also, the initiation efficiency was relatively constant above a certain initial catalyst concentration (10 ppm), and below this threshold concentration, the initiation efficiency dropped with decreasing catalyst concentrations.

ACS Macro Letters

Letter

Table 1. Result of Syntheses of SiO2-g-PMMA Particle Brushes

entry ^a	$[CuBr_2]_0^b$ (ppm)	reaction time (h)	conv ^c (%)	$M_{\rm n}^{d}$	$M_{ m w}/{M_{ m n}}^d$	f_{ino}^{e} (%)	$\sigma^f (\text{nm}^{-2})$
PMMA-1	400	2	7.9	42090	1.18	11.2	0.62
PMMA-2	200	2	9.0	41950	1.18	9.9	0.71
PMMA-3	100	2	11.8	60050	1.16	7.8	0.65
PMMA-4	50	1	7.2	38190	1.32	12.2	0.62
PMMA-5	25	1.5	10.7	56750	1.33	8.6	0.62
PMMA-6	10	1.5	3.7	78710	1.46	21.4	0.15
PMMA-7	5	1	3.9	108100	1.46	20.2	0.12
PMMA-8	2	1	3.4	86810	1.66	22.5	0.13
PMMA-9	1	1	2.5	181000	1.87	28.3	0.046
PMMA-10	0.5	1	3.7	247100	1.90	21.4	0.049
PMMA-11	0.2	1	1.3	296200	1.97	42.6	0.015
PMMA-12	0.1	1.5	2.2	229500	2.15	31.5	0.031
PMMA-13	0.05	1	0.55	149300	1.94	64.3	0.012
PMMA-14	0.02	1.5	1.9	223400	2.11	34.6	0.028
PMMA-15	0.01	1	1	197200	2.06	52.5	0.015

"Reaction condition: PMMA-1~15: $[MMA]_0/[SiO_2-Br]_0/[CuBr_2]_0/[Me_6TREN]_0$: $[Sn(EH)_2]_0 = 5000$: 1:x:10x:2.5, x=2/1/0.5/0.25/0.125/0.05/0.025/0.01/0.005/0.0025/0.001/0.0005/0.00025/0.001/0.0005 with 50 vol % anisole, at 60 °C, $[MMA]_0 = 4.7$ M. *Molar ratio vs monomer. Determined by gravimetric analysis. *Determined by SEC. *Fraction of inorganic content determined by TGA. *fCalculated from eq S1 according to TGA data.

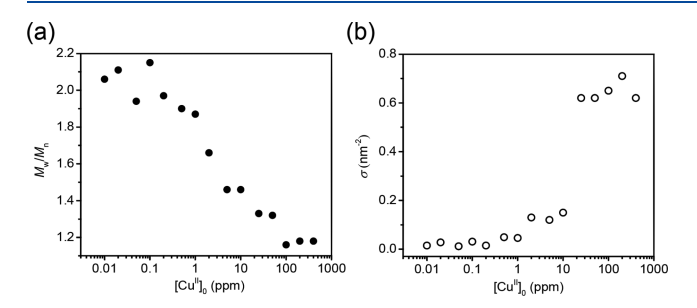


Figure 2. Reaction characteristics in the synthesis of SiO₂-g-PMMA particle brushes by ARGET ATRP with different $[Cu^{II}]_0$: (a) dispersity (M_w/M_n) vs $[Cu^{II}]_0$, (b) grafting density (σ) vs $[Cu^{II}]_0$.

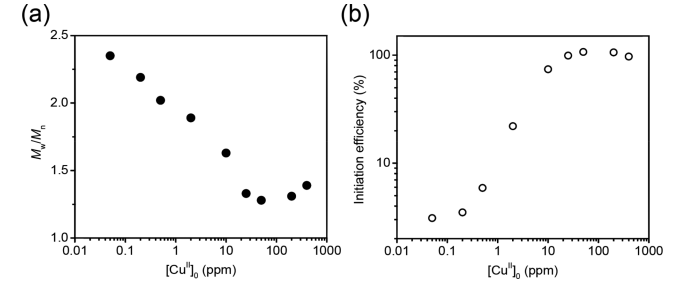


Figure 3. Reaction characteristics in the synthesis of linear PMMA homopolymers by ARGET ATRP with different $[Cu^{II}]_0$: (a) dispersity (M_w/M_n) vs $[Cu^{II}]_0$, (b) initiation efficiency vs $[Cu^{II}]_0$.

Figure 4a displays the semilogarithmic kinetic plots of model polymerization for linear MMA at different initial catalyst concentrations and indicates that the rate of polymerization is faster with a higher initial catalyst concentration. The apparent rate constant of polymerization, $k_{\rm p}^{\rm app}$, was calculated by eq S2, and a trend between the rate and the initial catalyst concentration is shown in Figure S1, the literature values of

propagation rate constant $k_{\rm p,MMA}$ = 833 M⁻¹ s⁻¹ at 60 °C was used to calculate the radical concentration, Figure S2.^{43,44} The polymerization rate of a classic ARGET ATRP reaction is defined by the ratio of the rates of reduction of Cu^{II}/L to Cu^I/L and radical termination. Thus, the overall rate should obey 1/2 order in both [RA] and [Cu^{II}/L].^{41,45} Figure S1 shows PMMA particle brushes polymerization rate indeed follows the

Table 2. Result of Syntheses of Linear PMMA

entry ^a	$[CuBr_2]_0^b$ (ppm)	reaction time (h)	conv ^c (%)	$M_{ m n,SEC}^{d}$	$M_{ m w}/{M_{ m n}}^d$	$M_{ m n,theo}^{e}$	efficiency ^f (%)
PMMA-L1	400	3	27.43	141700	1.39	137150	97
PMMA-L2	200	3	20.21	94640	1.31	101050	107
PMMA-L3	50	5	25.64	118950	1.28	128200	108
PMMA-L4	25	5	18.44	87350	1.33	92200	106
PMMA-L5	10	5	11.85	80980	1.63	59250	73
PMMA-L6	2	5	4.61	103800	1.89	23050	22
PMMA-L7	0.5	5	3.1	262200	2.02	15500	5.9
PMMA-L8	0.2	5	2.3	325300	2.19	11550	3.6
PMMA-L9	0.05	5	1.6	267000	2.35	8050	3.1

^aReaction condition: PMMA-L1~9: [MMA]₀/[EBiB]₀/[CuBr₂]₀/[Me₆TREN]₀:[Sn(EH)₂]₀ = 5000:1:x:10x:0.25, x = 2/1/0.25/0.125/0.05/0.01/0.0025/0.001/0.00025 with 50 vol % anisole, at 60 °C, [MMA]₀ = 4.7 M. ^bMolar ratio vs monomer. ^cDetermined by gravimetric analysis. ^dDetermined by SEC. ^eDetermined by conversion and target DP. ^fInitiation efficiency was calculated by $M_{\rm n,theo}/M_{\rm n,SEC}$.

ACS Macro Letters

Letter

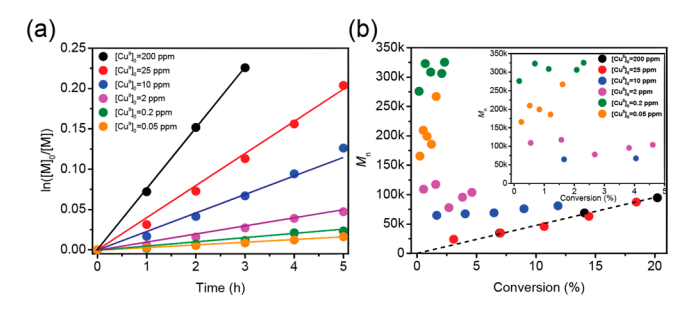


Figure 4. Results for linear homopolymer polymerization of methyl methacrylate (MMA) by ARGET ATRP under reaction condition: $[MMA]_0/[EBiB]_0/[CuBr_2]_0/[Me_6TREN]_0$: $[Sn(EH)_2]_0 = 5000:1:x:10x:2.5$, x = 1/0.125/0.05/0.01/0.001/0.00025, with 50 vol % anisole, at 60 °C: (a) Semilogarithmic kinetic plots for linear PMMA system; (b) Number-average molecular weight (M_n) vs conversion of linear PMMA, dash line in (b) show the theoretical M_n vs conversion plots under high $[Cu^{II}/L]_0$ conditions.

ARGET kinetics and the reaction order in Cu^{II}/L has a slope of 0.47. The initial concentration of the catalyst also significantly affected the dispersity (control) of polymers formed in the reactions. The dispersity (M_w/M_p) increased with decreasing [CuII/L]₀, up to 2.35, Figure S3. Figure 4b shows the correlations between number-average molecular weight and conversion with selected initial catalyst concentrations. An approximation of typical living polymerization features was observed for conditions with catalyst concentrations between 200 and 25 ppm [Cu^{II}/L]₀, and molecular weight showed good correlation with the theoretical value. However, when $[Cu^{II}/L]_0$ was decreased below 10 ppm, Figure 2b inset, control of polymerization was lost, as the relations between the molecular weight and conversion were no longer monotonically increasing. The 10 ppm [Cu^{II}/L]₀ concentration was also the transition point to a lower initiation

The PMMA chains generated in linear homopolymer system were initiated from ATRP initiator EBiB which is consistent with the observations for the SiO2-g-PMMA particle brush system. To confirm this, three control experiments were conducted. A Cu-free system ($[Cu^{II}/L]_0 = 0$ ppm, $[EBiB]_0 =$ 200 ppm, $[Sn(EH)_2]_0 = 400$ ppm), an initiator-free system $([Cu^{II}/L]_0 = 200 \text{ ppm}, [EBiB]_0 = 0 \text{ ppm}, [Sn(EH)_2]_0 = 400$ ppm), and the one with a Cu-and-initiator-free system ([CuII/ $L_{0}^{2} = 0$ ppm, $[EBiB]_{0}^{2} = 0$ ppm, $[Sn(EH)_{2}]_{0}^{2} = 400$ ppm). Kinetic studies, Figure S4, show that no polymerization occurred under the initiator-free and the initiator-and-Cufree conditions, but a slow uncontrolled polymerization proceeded under the Cu-free condition. Therefore, the mechanism of the polymerization of linear PMMA with different catalyst concentration can be summarized as predominantly a controlled radical polymerization above the critical initial catalyst concentration 10 ppm [CuII/L]0, for the current study conditions. The reactions showed good control, while the initiation efficiencies were high and independent of reaction time. When the initial catalyst concentration was below the critical threshold of 10 ppm, the reactions showed nonlinear correlations of M_n versus conversion and a slow initiation, due to insufficient deactivation, Figure S5. Specifically, in this linear polymerization study, the initiation efficiency was observed to decrease with decreasing initial catalyst concentration at the same reaction time. This

mechanism is believed to be applicable also to the particle brush system.

In conclusion, SiO₂-g-PMMA particle brushes were synthesized via ARGET ATRP with different initial catalyst concentrations and provided facile control of dispersity and grafting density. Under high catalyst concentration conditions (>10 ppm), the high grafting densities of the products were observed with uniform structures and the molecular weight distribution increased with decreasing [Cu^{II}/L]₀. When the initial catalyst concentration decreased to <10 ppm, the dispersity further increased, up to 2.3, and the grafting density dropped significantly, to as low as 0.012 chain/nm². Sparsely grafted particle brushes with large dispersity were obtained under these conditions, resulting in anisotropic string-like structures for the final product. The results of linear polymerization of MMA showed very similar trends in the initiation efficiency and the dispersity vs [Cu^{II}/L]₀. A transition from controlled to uncontrolled radical polymerization was revealed at initial catalyst concentrations below 10 ppm. Distinctly different types of control over the polymerization were observed above and below this critical concentration. Such observations demonstrated polymer brushes with a wide selection of MWD are accessible via tuned catalyst concentrations. This enables applications of these polymer brushes where a broad transition among polymer brush interactions is needed, such as antifouling, mechanical reinforcement, sensing, and separations.

ASSOCIATED CONTENT

S Supporting Information

The Supporting Information is available free of charge on the ACS Publications website at DOI: 10.1021/acsmacrolett.9b00405.

Experimental details and supporting figures (PDF)

AUTHOR INFORMATION

Corresponding Authors

*E-mail: bockstaller@cmu.edu. *E-mail: km3b@andrew.cmu.edu.

ORCID (

Jiajun Yan: 0000-0003-3286-3268 Sipei Li: 0000-0001-7659-1001

Michael R. Bockstaller: 0000-0001-9046-9539 Krzysztof Matyjaszewski: 0000-0003-1960-3402

Present Address

§Materials Science Division, Lawrence Berkeley National Laboratory, One Cyclotron Road, Berkeley, California 94720, United States.

Author Contributions

[‡]Z.W. and J.Y. contributed equally.

Author Contributions

Z.W. and J.Y. synthesized materials and performed characterization work. T.L, Q.W., and J.W. assisted in the synthesis; S.L. and M.O. assisted in the characterization work. M.R.B. and K.M. conceived and organized the project and, together with Z.W. and J.Y., wrote the manuscript.

Notes

The authors declare no competing financial interest.

ACS Macro Letters Letter

ACKNOWLEDGMENTS

This work was supported by NSF (DMR 1501324 and DMR 1410845) and the Department of Energy (DE-EE0006702), as well as the Scott Institute for Energy Technologies at Carnegie Mellon University.

REFERENCES

- (1) Qi, S.; Klushin, L. I.; Skvortsov, A. M.; Schmid, F. Polydisperse Polymer Brushes: Internal Structure, Critical Behavior, and Interaction with Flow. *Macromolecules* **2016**, *49* (24), 9665–9683.
- (2) Bixler, G. D.; Bhushan, B. Biofouling: lessons from nature. *Philos. Trans. R. Soc., A* **2012**, 370 (1967), 2381–2417.
- (3) Hui, C. M.; Pietrasik, J.; Schmitt, M.; Mahoney, C.; Choi, J.; Bockstaller, M. R.; Matyjaszewski, K. Surface-Initiated Polymerization as an Enabling Tool for Multifunctional (Nano-)Engineered Hybrid Materials. *Chem. Mater.* **2014**, *26* (1), 745–762.
- (4) Zoppe, J. O.; Ataman, N. C.; Mocny, P.; Wang, J.; Moraes, J.; Klok, H.-A. Surface-Initiated Controlled Radical Polymerization: State-of-the-Art, Opportunities, and Challenges in Surface and Interface Engineering with Polymer Brushes. *Chem. Rev.* **2017**, *117* (3), 1105–1318.
- (5) Barbey, R.; Lavanant, L.; Paripovic, D.; Schüwer, N.; Sugnaux, C.; Tugulu, S.; Klok, H.-A. Polymer Brushes via Surface-Initiated Controlled Radical Polymerization: Synthesis, Characterization, Properties, and Applications. *Chem. Rev.* **2009**, *109* (11), 5437–5527.
- (6) Kumar, S. K.; Benicewicz, B. C.; Vaia, R. A.; Winey, K. I. 50th Anniversary Perspective: Are Polymer Nanocomposites Practical for Applications? *Macromolecules* **2017**, *50* (3), 714–731.
- (7) Romeis, D.; Merlitz, H.; Sommer, J. U. A new numerical approach to dense polymer brushes and surface instabilities. *J. Chem. Phys.* **2012**, *136* (4), No. 044903.
- (8) Matyjaszewski, K.; Xia, J. Atom Transfer Radical Polymerization. Chem. Rev. 2001, 101 (9), 2921–2990.
- (9) Matyjaszewski, K. Advanced Materials by Atom Transfer Radical Polymerization. *Adv. Mater.* **2018**, *30* (23), 1706441.
- (10) Matyjaszewski, K. Atom Transfer Radical Polymerization (ATRP): Current Status and Future Perspectives. *Macromolecules* **2012**, 45 (10), 4015–4039.
- (11) Jakubowski, W.; Min, K.; Matyjaszewski, K. Activators Regenerated by Electron Transfer for Atom Transfer Radical Polymerization of Styrene. *Macromolecules* **2006**, *39* (1), 39–45.
- (12) Matyjaszewski, K.; Jakubowski, W.; Min, K.; Tang, W.; Huang, J.; Braunecker, W. A.; Tsarevsky, N. V. Diminishing catalyst concentration in atom transfer radical polymerization with reducing agents. *Proc. Natl. Acad. Sci. U. S. A.* **2006**, *103* (42), 15309–15314.
- (13) Tsarevsky, N. V.; Matyjaszewski, K. Green" Atom Transfer Radical Polymerization: From Process Design to Preparation of Well-Defined Environmentally Friendly Polymeric Materials. *Chem. Rev.* **2007**, *107* (6), 2270–2299.
- (14) Pan, X.; Fantin, M.; Yuan, F.; Matyjaszewski, K. Externally controlled atom transfer radical polymerization. *Chem. Soc. Rev.* **2018**, 47 (14), 5457–5490.
- (15) Milner, S. T.; Witten, T. A.; Cates, M. E. Effects of polydispersity in the end-grafted polymer brush. *Macromolecules* **1989**, 22 (2), 853–861.
- (16) Martin, T. B.; Dodd, P. M.; Jayaraman, A. Polydispersity for Tuning the Potential of Mean Force between Polymer Grafted Nanoparticles in a Polymer Matrix. *Phys. Rev. Lett.* **2013**, *110* (1), No. 018301.
- (17) de Vos, W. M.; Leermakers, F. A. M. Modeling the structure of a polydisperse polymer brush. *Polymer* **2009**, *50* (1), 305–316.
- (18) de Vos, W. M.; Leermakers, F. A. M.; de Keizer, A.; Kleijn, J. M.; Cohen Stuart, M. A. Interaction of Particles with a Polydisperse Brush: A Self-Consistent-Field Analysis. *Macromolecules* **2009**, 42 (15), 5881–5891.
- (19) Liu, X.; Wang, C.-G.; Goto, A. Polymer Dispersity Control by Organocatalyzed Living Radical Polymerization. *Angew. Chem., Int. Ed.* **2019**, 58, 5598.

- (20) Yadav, V.; Jaimes-Lizcano, Y. A.; Dewangan, N. K.; Park, N.; Li, T.-H.; Robertson, M. L.; Conrad, J. C. Tuning Bacterial Attachment and Detachment via the Thickness and Dispersity of a pH-Responsive Polymer Brush. *ACS Appl. Mater. Interfaces* **2017**, *9* (51), 44900–44910.
- (21) Yan, J.; Kristufek, T.; Schmitt, M.; Wang, Z.; Xie, G.; Dang, A.; Hui, C. M.; Pietrasik, J.; Bockstaller, M. R.; Matyjaszewski, K. Matrixfree Particle Brush System with Bimodal Molecular Weight Distribution Prepared by SI-ATRP. *Macromolecules* **2015**, 48 (22), 8208–8218.
- (22) Nair, N.; Wentzel, N.; Jayaraman, A. Effect of bidispersity in grafted chain length on grafted chain conformations and potential of mean force between polymer grafted nanoparticles in a homopolymer matrix. *J. Chem. Phys.* **2011**, *134* (19), 194906.
- (23) Rungta, A.; Natarajan, B.; Neely, T.; Dukes, D.; Schadler, L. S.; Benicewicz, B. C. Grafting Bimodal Polymer Brushes on Nanoparticles Using Controlled Radical Polymerization. *Macromolecules* **2012**, *45* (23), 9303–9311.
- (24) Natarajan, B.; Neely, T.; Rungta, A.; Benicewicz, B. C.; Schadler, L. S. Thermomechanical Properties of Bimodal Brush Modified Nanoparticle Composites. *Macromolecules* **2013**, *46* (12), 4909–4918.
- (25) Li, Y.; Krentz, T. M.; Wang, L.; Benicewicz, B. C.; Schadler, L. S. Ligand Engineering of Polymer Nanocomposites: From the Simple to the Complex. ACS Appl. Mater. Interfaces 2014, 6 (9), 6005–6021.
- (26) Jakubowski, W.; Matyjaszewski, K. Activators Regenerated by Electron Transfer for Atom-Transfer Radical Polymerization of (Meth)acrylates and Related Block Copolymers. *Angew. Chem., Int. Ed.* **2006**, 45 (27), 4482–4486.
- (27) Lamson, M.; Kopeć, M.; Ding, H.; Zhong, M.; Matyjaszewski, K. Synthesis of well-defined polyacrylonitrile by ICAR ATRP with low concentrations of catalyst. *J. Polym. Sci., Part A: Polym. Chem.* **2016**, 54 (13), 1961–1968.
- (28) Listak, J.; Jakubowski, W.; Mueller, L.; Plichta, A.; Matyjaszewski, K.; Bockstaller, M. R. Effect of Symmetry of Molecular Weight Distribution in Block Copolymers on Formation of "Metastable" Morphologies. *Macromolecules* **2008**, *41* (15), 5919–5927.
- (29) Mastan, E.; Xi, L.; Zhu, S. Factors Affecting Grafting Density in Surface-Initiated ATRP: A Simulation Study. *Macromol. Theory Simul.* **2016**, 25 (3), 220–228.
- (30) Riazi, H.; A. Shamsabadi, A.; Grady, M. C.; Rappe, A. M.; Soroush, M. Experimental and Theoretical Study of the Self-Initiation Reaction of Methyl Acrylate in Free-Radical Polymerization. *Ind. Eng. Chem. Res.* **2018**, *57* (2), 532–539.
- (31) Srinivasan, S.; Lee, M. W.; Grady, M. C.; Soroush, M.; Rappe, A. M. Self-Initiation Mechanism in Spontaneous Thermal Polymerization of Ethyl and n-Butyl Acrylate: A Theoretical Study. *J. Phys. Chem. A* **2010**, *114* (30), 7975–7983.
- (32) Hui, C. M.; Dang, A.; Chen, B.; Yan, J.; Konkolewicz, D.; He, H.; Ferebee, R.; Bockstaller, M. R.; Matyjaszewski, K. Effect of Thermal Self-Initiation on the Synthesis, Composition, and Properties of Particle Brush Materials. *Macromolecules* **2014**, *47* (16), 5501–5508.
- (33) Jiao, Y.; Tibbits, A.; Gillman, A.; Hsiao, M.-S.; Buskohl, P.; Drummy, L. F.; Vaia, R. A. Deformation Behavior of Polystyrene-Grafted Nanoparticle Assemblies with Low Grafting Density. *Macromolecules* **2018**, *51* (18), 7257–7265.
- (34) Jiao, Y.; Parra, J.; Akcora, P. Effect of Ionic Groups on Polymer-Grafted Magnetic Nanoparticle Assemblies. *Macromolecules* **2014**, *47* (6), 2030–2036.
- (35) Liu, S.; Senses, E.; Jiao, Y.; Narayanan, S.; Akcora, P. Structure and Entanglement Factors on Dynamics of Polymer-Grafted Nanoparticles. *ACS Macro Lett.* **2016**, 5 (5), 569–573.
- (36) Akcora, P.; Liu, H.; Kumar, S. K.; Moll, J.; Li, Y.; Benicewicz, B. C.; Schadler, L. S.; Acehan, D.; Panagiotopoulos, A. Z.; Pryamitsyn, V.; Ganesan, V.; Ilavsky, J.; Thiyagarajan, P.; Colby, R. H.; Douglas, J. F. Anisotropic self-assembly of spherical polymer-grafted nanoparticles. *Nat. Mater.* **2009**, *8*, 354.

ACS Macro Letters

(37) Zhao, D.; Di Nicola, M.; Khani, M. M.; Jestin, J.; Benicewicz, B. C.; Kumar, S. K. Self-Assembly of Monodisperse versus Bidisperse Polymer-Grafted Nanoparticles. *ACS Macro Lett.* **2016**, *5* (7), 790–795.

- (38) Zheng, Y.; Huang, Y.; Abbas, Z. M.; Benicewicz, B. C. One-pot synthesis of inorganic nanoparticle vesicles via surface-initiated polymerization-induced self-assembly. *Polym. Chem.* **2017**, *8* (2), 370–374.
- (39) Matyjaszewski, K. The importance of exchange reactions in controlled/living radical polymerization in the presence of alkoxyamines and transition metals. *Macromol. Symp.* **1996**, *111* (1), 47–61.
- (40) Krys, P.; Matyjaszewski, K. Kinetics of Atom Transfer Radical Polymerization. *Eur. Polym. J.* **2017**, *89*, 482–523.
- (41) Li, X.; Wang, W.-J.; Li, B.-G.; Zhu, S. Kinetics and Modeling of Solution ARGET ATRP of Styrene, Butyl Acrylate, and Methyl Methacrylate. *Macromol. React. Eng.* **2011**, 5 (9–10), 467–478.
- (42) Shipp, D. A.; Matyjaszewski, K. Kinetic Analysis of Controlled/ "Living" Radical Polymerizations by Simulations. 2. Apparent External Orders of Reactants in Atom Transfer Radical Polymerization. *Macromolecules* **2000**, *33* (5), 1553–1559.
- (43) Zhong, M.; Matyjaszewski, K. How Fast Can a CRP Be Conducted with Preserved Chain End Functionality? *Macromolecules* **2011**, 44 (8), 2668–2677.
- (44) Buback, M.; Kurz, C. H.; Schmaltz, C. Pressure dependence of propagation rate coefficients in free-radical homopolymerizations of methyl acrylate and dodecyl acrylate. *Macromol. Chem. Phys.* **1998**, 199 (8), 1721–1727.
- (45) Keating, J. J., IV; Lee, A.; Belfort, G. Predictive Tool for Design and Analysis of ARGET ATRP Grafting Reactions. *Macromolecules* **2017**, *50* (20), 7930–7939.